

Cite this: *New J. Chem.*, 2011, **35**, 2691–2696

www.rsc.org/njc

PAPER

# Ruthenium(II) and rhodium(III) porphyrin phosphine complexes: influence of substitution pattern on structure and electronic properties†

Andrew D. Bond,<sup>a</sup> Jeremy K. M. Sanders<sup>b</sup> and Eugen Stulz<sup>\*c</sup>

Received (in Victoria, Australia) 8th July 2011, Accepted 18th August 2011

DOI: 10.1039/c1nj20598f

A series of ruthenium(II) and rhodium(III) porphyrin complexes with diphenyl phenylacetylene phosphine (dpap) was synthesised and fully characterised by UV-vis, <sup>1</sup>H NMR and <sup>31</sup>P{<sup>1</sup>H} NMR spectroscopy, and in most cases also by single-crystal X-ray diffraction. The substitution pattern of the porphyrin was varied with increasing *meso*-phenyl substitution, from octa-ethyl porphyrin (OEP), through diphenyl di-ethyl porphyrin (DPP), to tetraphenyl porphyrin (TPP) and 3,5-di-<sup>t</sup>butyl tetraphenyl porphyrin (tbTPP). The dpap readily displaces the CO ligand from the parent Ru(CO)(porphyrin) and the iodide from the Rh(I)(porphyrin) to give bis-phosphine complexes M(dpap)<sub>2</sub>(porphyrin). The UV-vis spectra reveal that some of the complexes are partially dissociated at concentrations of 10<sup>-6</sup> M, and the association constants were estimated to be in the range of 10<sup>6</sup> to 10<sup>7</sup> M<sup>-1</sup> for the first, and 10<sup>4</sup> to 10<sup>6</sup> M<sup>-1</sup> for the second binding event. The <sup>1</sup>H NMR chemical shifts of the complexes vary greatly despite the fact that they display very similar geometries in the solid state, and no correlation could be discerned between the crystal structures and the spectroscopic parameters in solution.

## Introduction

Ruthenium and rhodium porphyrins have attracted considerable interest in the recent years due to their characteristic electronic properties, which make them suitable model compounds in artificial photosynthesis and catalysis. The iso-electronic low-spin Fe(II) porphyrins are widely present in nature, in particular as heme complexes (P450). The iron-heme complex is liable to oxidation, readily forming inactive iron-oxo dimers, which is a major issue when using iron-porphyrins to study their catalytic activity. The use of ruthenium eliminates this problem, hence Ru(II) porphyrins have generally been employed as P450 model compounds for the study of bio-mimetic oxidation reactions,<sup>1</sup> as catalysts in hydrocarbon oxidation,<sup>2,3</sup> as catalysts for amidation<sup>4</sup> and cycloaddition<sup>5</sup> reactions, and in photoinduced electron transfer reactions.<sup>6</sup> Ru(II) porphyrin and phthalocyanine complexes with primary and secondary phosphines were reported for phosphine functionalization and

phosphinidene transfer reactions.<sup>7,8</sup> Likewise, Rh(III) porphyrins have been studied in metallo radical chemistry<sup>9</sup> and in olefin hydrofunctionalisation,<sup>10</sup> although these complexes are far less commonly studied. More exotic ligands such as charged phosphoranido ligands on Rh(III) porphyrins have also been reported.<sup>11</sup>

Utilising the axial coordination chemistry of metallo porphyrins is a useful strategy to create supramolecular porphyrin assemblies.<sup>12</sup> As for many other metallo porphyrins, both Ru- and Rh-porphyrins can readily form stable five- and six-coordinate complexes with nitrogen, sulfur and phosphorus donor ligands. In particular, phosphine ligands are attractive for the construction of supramolecular assemblies because the association constants are high, in the range of 10<sup>6</sup> to 10<sup>8</sup> M<sup>-1</sup>,<sup>13–15</sup> and are orthogonal to Zn-nitrogen and Sn-oxygen complexes.<sup>16–18</sup> We have exploited this coordination chemistry to create supramolecular multi-porphyrin arrays.<sup>19–21</sup> The bonding, however, is not kinetically inert, and the ligand exchange can be used to create dynamic combinatorial libraries.<sup>22,23</sup> Other examples of Ru- and Rh-porphyrin phosphine complexes in supramolecular assemblies are scarce, and normally nitrogen complexation is favoured for the creation of supramolecular assemblies with either ruthenium<sup>24–27</sup> or rhodium<sup>28</sup> porphyrins, in particular also making use of the reversible coordination to create dynamic switching systems.<sup>29,30</sup>

We have studied the coordination chemistry of various P(III) ligands with both ruthenium and rhodium porphyrins,<sup>13–15</sup> *i.e.* PPh<sub>3</sub>, phenyl-acetylene phosphines and phosphonites, as model compounds for more complex supramolecular systems. We found that a diphenyl phosphine with an acetylene

<sup>a</sup> Department of Physics and Chemistry, University of Southern Denmark, Campusvej 55, 5230 Odense M, Denmark.

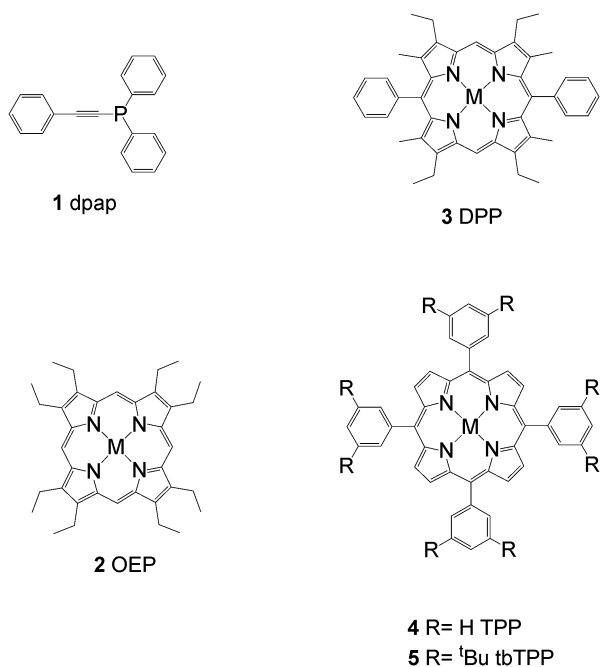
E-mail: adb@chem.sdu.dk

<sup>b</sup> University Chemical Laboratory, University of Cambridge, Lensfield Rd, Cambridge CB2 1EW, UK. E-mail: jkms@cam.ac.uk

<sup>c</sup> School of Chemistry, University of Southampton, Highfield, Southampton SO17 2HU, UK. E-mail: est@soton.ac.uk;

Fax: + 44 (0)23 8059 3131; Tel: + 44 (0)23 8059 9369

† Electronic supplementary information (ESI) available: Spectroscopic analyses of the complexes. CCDC reference numbers 834653–834657. For ESI and crystallographic data in CIF or other electronic format see DOI: 10.1039/c1nj20598f.



**Scheme 1** Structures of the phosphine ligand **1** and of the metalloporphyrins **2–5**. M = Ru(II) or Rh(III)

phosphine substituent as synthon is most suitable from both a synthetic and stability point of view; the stability is most likely a combination of steric and electronic factors. Supramolecular building blocks containing acetylenes are usually readily available, and transformation into the corresponding phosphine is straightforward using chloro-diphenyl phosphine. Here, we report on the influence of the porphyrin substitution pattern on the structural and electronic properties of complexes with diphenyl phenyl-acetylene phosphine (**1**, Scheme 1). To our knowledge, no systematic study involving different Ru- and Rh-porphyrins with one specific phosphine ligand has been reported. This, however, is important in order to be able to make predictions for the suitability of a phosphine porphyrin complex for a particular application such as in catalysis or supramolecular chemistry. We have varied the porphyrin structure with respect to its substitution pattern with increasing *meso*-phenyl substituents, from octaethylporphyrin (**2**, OEP), through diphenylporphyrin (**3**, DPP) to tetraphenylporphyrin (**4**, TPP) and tetra(*di*-*tert*-butyl-phenyl)porphyrin (**5**, dtbTPP). The octahedral di-phosphine complexes (dpap)<sub>2</sub>M(porphyrin) have been prepared, and their spectroscopic properties are evaluated using absorption and NMR spectroscopy. One of the structures (**P<sub>2</sub>-Rh4**) obtained from single crystal X-ray diffraction (XRD) has been published elsewhere,<sup>13</sup> as have the structures of some related complexes of dpap with a rhodium di(*di*-*tert*-butyl-phenyl) porphyrin.<sup>15</sup> However, the majority of the crystal structures have not been reported previously and are included in this paper.

## Results and discussion

### Synthesis and UV-vis spectroscopy

The synthesis and characterisation of dpap (**1**)<sup>31</sup> and of the metalloporphyrins **Ru2** to **Ru5** and **Rh2** to **Rh5** has been

described previously.<sup>19</sup> The bis-phosphine complexes of the Ru- and Rh-porphyrins, denoted **P<sub>2</sub>-RuX** or **P<sub>2</sub>-RhX**, are readily available as reported earlier.<sup>13,15</sup> Generally, it is sufficient to mix the porphyrins with two equivalents of **1** in DCM, and after evaporation of the solvent the pure complexes can be obtained by re-crystallisation from DCM-MeOH. Other methods to obtain phosphine complexes of **Rh4** have also been reported.<sup>32</sup>

UV-vis spectroscopy is very diagnostic for ligand complexation in metallo-porphyrins, since porphyrins show very characteristic absorbance spectra (Fig. 1). These are dominated by a strong B-band (Soret band) absorption at around 400–420 nm, and weaker Q-band absorptions at higher wavelengths (500–700 nm, Table 1). Upon ligand complexation, the absorbances typically shift to higher wavelengths by about 10–40 nm, which is diagnostic and can be used to monitor the binding event. Solutions of the re-dissolved rhodium complexes in DCM show absorbance spectra characteristic for fully intact complexes at  $c = 5 \times 10^{-6}$  M because the B-band absorbances appear sharp; an exception is **P<sub>2</sub>-Rh5** where a small shoulder can be observed at around 426 nm. Overall, the spectra are consistent with earlier experiments where the association constant of **P<sub>2</sub>-Rh4** was determined to be  $K_a = 4.6 \times 10^4$  M<sup>-1</sup>,<sup>13</sup> and the association constants in the present series were determined to be in the same order (Table 1). The complexes of the Ru-series, on the other hand, do not show sharp porphyrin absorbances, but shoulders, as in the case of **P-Ru5**, or even two distinct absorbance maxima as in **P-Ru2**. This indicates that these complexes dissociate partially at this concentration. As reported earlier, the  $K_a$ -values for the ruthenium complexes are about one order of magnitude lower compared to the rhodium complexes.<sup>15</sup> At lower concentrations, the rhodium series also shows dissociation, and the B-band absorbances can be de-convoluted into three distinct bands corresponding to the free porphyrin, the mono-phosphine and the bis-phosphine complexes (see ESI). From this, association constants can be determined.<sup>15</sup> The data show that the phosphine complex with **Ru2** is the weakest complex and dissociates readily at

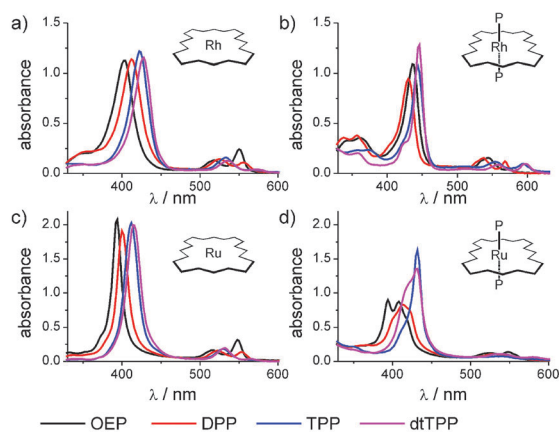


**Fig. 1** UV-vis spectra of the porphyrin complexes;  $c = 5 \times 10^{-6}$  M in DCM. (a) Rh-porphyrins; (b) Rh-bisphosphine complexes; (c) Ru-porphyrins; (d) Ru-bisphosphine complexes.

**Table 1** Spectroscopic data for the porphyrin complexes

Complex	$K_{a1}/[M^{-1}]$	$K_{a2}/[M^{-1}]$	$\lambda_{\max}/[\text{nm}]$ porphyrin	$\lambda_{\max}/[\text{nm}]P_1$ -complex	$\lambda_{\max}/[\text{nm}]P_2$ -complex
<b>P<sub>2</sub>-Rh2</b>	$2.0 \times 10^7$	$4.8 \times 10^5$	404, 518, 550	426, 499	434, 538, 575
<b>P<sub>2</sub>-Rh3</b>	$1.7 \times 10^7$	$8.4 \times 10^5$	412, 526, 556	430, 488	438, 537, 568
<b>P<sub>2</sub>-Rh4</b>	$3.0 \times 10^7$ <sup>a</sup>	$4.6 \times 10^4$ <sup>a</sup>	422, 533, 566	437, 504	445, 557, 596
<b>P<sub>2</sub>-Rh5</b>	$9.3 \times 10^5$	$6.3 \times 10^6$	428, 534, 572	435, 515	445, 562, 597
<b>P<sub>2</sub>-Ru2</b>	$3.4 \times 10^5$	$9.2 \times 10^4$	394, 516, 548	407, 528, 558	418
<b>P<sub>2</sub>-Ru3</b>	$2.5 \times 10^5$	$1.9 \times 10^5$	400, 522, 554	411, 536, 567	421
<b>P<sub>2</sub>-Ru4</b>	$4.0 \times 10^7$	$8.2 \times 10^5$	412, 530, 560	426	432
<b>P<sub>2</sub>-Ru5</b>	$1.4 \times 10^7$	$3.5 \times 10^5$	414, 532, 566	425, 546, 581	433

<sup>a</sup> Data from ref. 13; P<sub>1</sub>-complex and P<sub>2</sub>-complex denote mono- and bis-phosphine complexes.

concentrations where the **P<sub>2</sub>-Ru4** complex is still largely intact. This difference in complex stability can most probably be attributed to the electronics of the porphyrins. The lower stability of the complex in **P<sub>2</sub>-Ru5** compared to **P<sub>2</sub>-Ru4** is more likely to arise from a steric influence of the additional *tert*-butyl groups on the *meso*-phenyl substituents. In the rhodium series, **P<sub>2</sub>-Rh4** seems to be the least stable complex.

### NMR spectroscopy

Since the ruthenium and rhodium metallo-porphyrins are diamagnetic, both <sup>1</sup>H NMR and <sup>31</sup>P{<sup>1</sup>H} NMR spectroscopy can be used to ascertain the integrity of the complexes. It should be noted that at the concentrations used for NMR spectroscopy (1–5 mM) the complexes are fully associated at room temperature which is different from the low concentration UV-vis measurements, where the complexes may dissociate. We have discussed the NMR studies of the kinetic lability and ligand exchange reactions of both phosphine-ruthenium and rhodium porphyrin complexes previously.<sup>13,15</sup> Analogously, in the complexes here ligand exchange is slow on the NMR time scale, and the chemical shifts represent the associated complexes which are concentration independent. In the <sup>1</sup>H NMR spectra, the most characteristic chemical shifts indicative of complex formation are observed for the phenyl substituents on phosphorus (Fig. 2). Due to their positioning above the shielding region of the porphyrin, the resonances appear upfield shifted. The *tb*TPP-complexes are generally very poorly soluble in CDCl<sub>3</sub>, therefore the spectra appear very noisy for **P<sub>2</sub>-Ru5** and **P<sub>2</sub>-Rh5** even in the presence of 10% CD<sub>3</sub>OD. The <sup>31</sup>P{<sup>1</sup>H} NMR chemical shifts (Table 2) are indicative of the composition of the complex, *i.e.* if the metal is coordinated by one phosphine or by two. The <sup>31</sup>P{<sup>1</sup>H} NMR chemical shifts of the mono-phosphine complexes were obtained by adding one equivalent of the ligand to the porphyrin solution. These complexes can, however, not be isolated due to the lability of the carbonyl or iodide ligand on the ruthenium and rhodium, respectively.<sup>13,15</sup> The chemical shifts are consistent with previous measurements of similar complexes, and do not show any particular trends within the porphyrin series; in fact, they vary only by a few ppm within the rhodium or ruthenium series. Hence, the differences in chemical shifts as observed by <sup>1</sup>H NMR spectroscopy are not observed for the phosphorus nucleus.

Interestingly, the ruthenium and rhodium phosphine complexes show quite different chemical shifts for the phenyl protons in the *ortho*, *meta* and *para* positions. Two trends can be seen

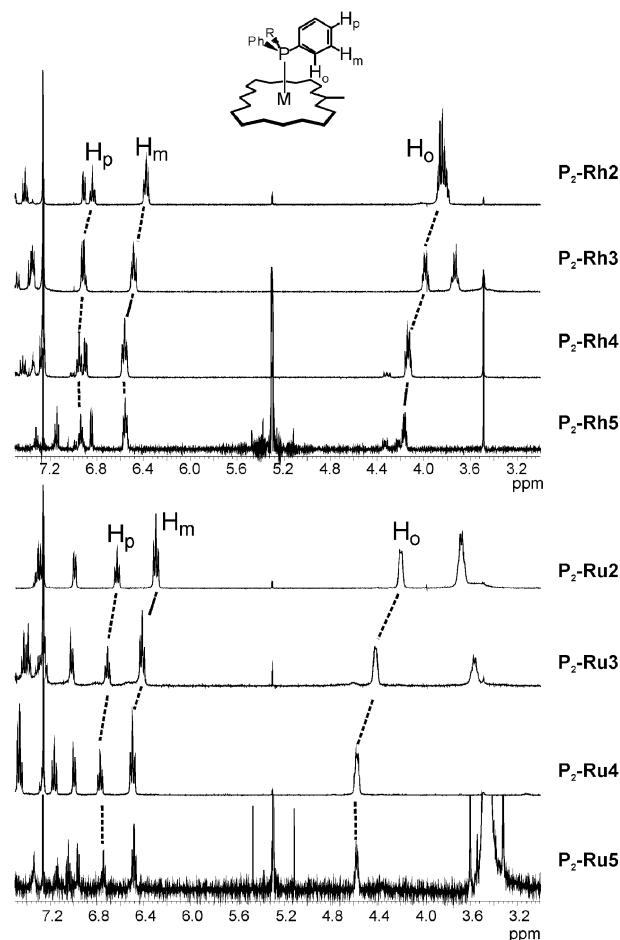


**Fig. 2** Part of the <sup>1</sup>H NMR spectra displaying the chemical shift differences in the bis-dpp complexes.

when comparing the different complexes. First, the shift differences from the free phosphine to the complexed ligand vary with porphyrin structure, with OEP (**2**) showing the largest shift and TPP/*tb*TPP (**4/5**) showing the smallest shifts (Fig. 2). This is not in line with the binding constants, where the OEP complexes normally show smaller  $K_a$  values than TPP complexes. However, additional shielding or deshielding effects arising from the *meso*-phenyl substituents must be taken into account; these would explain the differences observed with increasing number of *meso*-phenyl groups. Second, the *ortho* protons in the ruthenium series show a smaller high-field shift, whereas the *meta* and *para* protons show a larger shift compared to the

**Table 2** NMR data of the porphyrin complexes

Complex	$\delta^{31}\text{P}/[\text{ppm}] (J_{\text{Rh-P}}/[\text{Hz}])^a$		$\delta^1\text{H}/[\text{ppm}]$		
	P <sub>1</sub> -complex	P <sub>2</sub> -complex	H <sub>o</sub>	H <sub>m</sub>	H <sub>p</sub>
<b>P<sub>2</sub>-Rh2</b>	-7 (119)	-9 (88)	3.82	6.36	6.83
<b>P<sub>2</sub>-Rh3</b>	-8 (118)	-10 (89)	3.99	6.47	6.91
<b>P<sub>2</sub>-Rh4</b>	-9 (115)	-9 (87)	4.14	6.56	6.95
<b>P<sub>2</sub>-Rh5</b>	-7 (114)	-8 (85)	4.18	6.58	6.96
<b>P<sub>2</sub>-Ru2</b>	-15	-1	4.2	6.29	6.63
<b>P<sub>2</sub>-Ru3</b>	-14	2	4.41	6.41	6.7
<b>P<sub>2</sub>-Ru4</b>	-12	0	4.57	6.5	6.77
<b>P<sub>2</sub>-Ru5</b>	-11	3	4.6	6.5	6.76

<sup>a</sup> dpap:  $\delta$  -32 ppm.

rhodium series. This is best demonstrated in the overlay of the partial <sup>1</sup>H NMR spectra of the DPP (**2**) complexes (Fig. 3).

From a structural point of view, the XRD structures do not show large variations in the relative geometries, *i.e.* the distances of the protons to the porphyrin plane are comparable, at least in the solid state (*vide infra* and inset in Fig. 3). Also, the symmetry seen in the <sup>1</sup>H NMR spectra indicate relatively unhindered rotation of the metal-phosphorus bonds and of the phenyl groups. Since the differences in chemical shift cannot be assigned to the geometry or the presence of the *meso*-phenyl groups (as the number is the same in the corresponding complex), the electronics in the individual complexes must be quite different. It seems that the de-shielding effect is large for rhodium on the *ortho* protons (close to the porphyrin plane) but weak on the *para* protons (further away from the porphyrin plane). This raises the question as to whether the magnetic fields induced through the ring currents are strongly influenced by the metals, and whether this magnetic field can have magnitudes that vary strongly with distance from the porphyrin planes depending on the metal. Generally it is accepted that porphyrins have similar to identical ring currents, unless they are structurally distorted.<sup>33,34</sup> However, the differences seen in the absorbances indicate changes in the energy splitting of the ground and excited states. Also, calculations on free-base and Mg porphine show that metallation can have an effect on the ring current of the porphyrin.<sup>35</sup> The  $\sigma$ - and  $\pi$ -effects of the metal should also be considered. The question about the origin of these unusual chemical shift effects might be answered with computational methods, which are beyond our current scope.

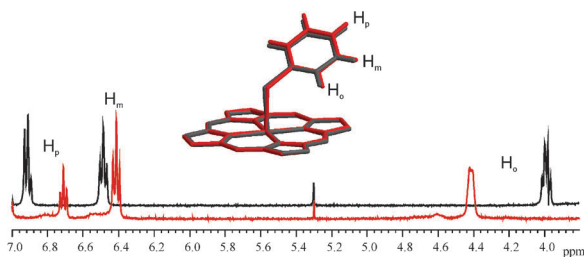


**Fig. 3** Part of the <sup>1</sup>H NMR spectra of **P<sub>2</sub>-Rh2** (black) and **P<sub>2</sub>-Ru2** (red) displaying the chemical shifts of the phosphine-phenyl group. The overlaid structures are taken from the XRD structures; other substituents on the DPP and dpap are omitted for clarity.

## Single-crystal X-ray diffraction

The X-ray crystal structure of **P<sub>2</sub>-Rh4** has been reported previously.<sup>13</sup> The structures of **P<sub>2</sub>-Rh2** and **P<sub>2</sub>-Ru5** have not been satisfactorily determined to date. Crystallographic data for the remaining five complexes are summarised in Table 3. The molecular units are shown in Fig. 4, and selected geometrical parameters are summarised in Table 4. Except for **P<sub>2</sub>-Ru4**, all of the porphyrin complexes lie on crystallographic inversion centres. **P<sub>2</sub>-Ru4** contains two independent complexes, one lying on an inversion centre and one on a general position. The two complexes exhibit different orientations of the dpap ligands with respect to the porphyrin core (described below). The former exhibits disorder for one phenyl substituent on P, modelled in two orientations related by rotation of *ca* 30° about the P-C(*ipso*) bond. For **P<sub>2</sub>-Rh5**, there is one porphyrin complex per unit cell in space group *P* $\bar{1}$ . The single iodide site in the unit cell was refined with 50% site occupancy, consistent with charge balance. Additional electron density in this region could be modelled satisfactorily as a pentane molecule having 50% site occupancy. Thus, there is one iodide anion and one pentane molecule per unit cell (*i.e.* per **P<sub>2</sub>-Rh5** complex). In **P<sub>2</sub>-Ru3**, the chloroform molecule is disordered about a crystallographic inversion centre.

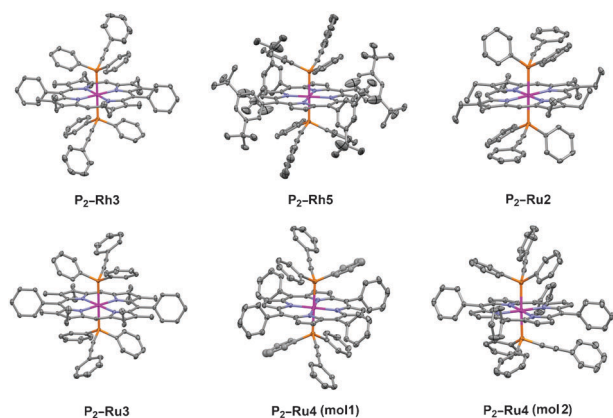
In all determined structures within the series (including **P<sub>2</sub>-Rh4**<sup>13</sup>) the porphyrins are essentially flat, and the M–P and M–N bond distances are closely comparable (Table 4). In **P<sub>2</sub>-Ru2** and **P<sub>2</sub>-Rh3/Ru3**, the acetylenic arm of dpap lies over the unsubstituted *meso* positions of the porphyrin and the phenyl substituents on P lie above the pyrrole rings (Fig. 4). In **P<sub>2</sub>-Rh4/Ru4** and **P<sub>2</sub>-Rh5**, the dpap ligand is rotated by *ca* 45° from this orientation so that the acetylenic arm lies over one pyrrole ring, one phenyl substituent lies over another pyrrole ring and the other phenyl substituent lies over one *meso* position of the porphyrin. In **P<sub>2</sub>-Ru4**, the non-centrosymmetric complex has similar orientations for the acetylenic arms of the two dpap ligands, but they are rotated *ca* 90° to each other viewed in projection along the P–Ru–P axis.

## Conclusions

We have analysed a range of ruthenium and rhodium porphyrin bis-phosphine complexes, which are readily available by ligand displacement on the parent porphyrins. The weaker second binding of the phosphine indicates that one ligand can be displaced preferentially and potentially be substituted with another ligand. This is of importance in catalysis applications where efficient ligand exchange is crucial. The electronic parameters vary greatly in the different complexes, in particular the absorbances change within the series of porphyrins. <sup>1</sup>H NMR spectra reveal that the shielding effects are more complex than might be expected, and the differences cannot easily be explained from structural aspects. It is evident that more electronic parameters have to be taken into account, in particular arising from metallation of the porphyrin. More quantum mechanical analyses are thus required to understand fully the electronic behaviour of metallo porphyrins and their complexes, in particular their activity towards substrates in catalysis.

**Table 3** Selected crystallographic data for **P<sub>2</sub>-Rh3**, **P<sub>2</sub>-Rh5**, **P<sub>2</sub>-Ru2**, **P<sub>2</sub>-Ru3** and **P<sub>2</sub>-Ru4**

	<b>P<sub>2</sub>-Rh3</b>	<b>P<sub>2</sub>-Rh5</b>	<b>P<sub>2</sub>-Ru2</b>	<b>P<sub>2</sub>-Ru3</b>	<b>P<sub>2</sub>-Ru4</b>
Empirical formula	[C <sub>84</sub> H <sub>74</sub> N <sub>4</sub> P <sub>2</sub> Rh] <sup>+</sup> I <sup>-</sup> ·CH <sub>2</sub> Cl <sub>2</sub>	[C <sub>116</sub> H <sub>122</sub> N <sub>4</sub> P <sub>2</sub> Rh] <sup>+</sup> I <sup>-</sup> ·C <sub>5</sub> H <sub>12</sub>	C <sub>76</sub> H <sub>74</sub> N <sub>4</sub> P <sub>2</sub> Ru	C <sub>84</sub> H <sub>74</sub> N <sub>4</sub> P <sub>2</sub> Ru·CHCl <sub>3</sub>	C <sub>84</sub> H <sub>58</sub> N <sub>4</sub> P <sub>2</sub> Ru
Formula weight	1516.15	1936.07	1206.40	1421.85	1286.35
Crystal system	Monoclinic	Triclinic	Triclinic	Triclinic	Monoclinic
Space group	C2/c	P1	P1	P1	C2/c
T/K	180(2)	220(2)	180(2)	180(2)	180(2)
a/Å	26.5305(5)	12.0257(3)	11.5833(3)	11.0429(2)	23.5610(2)
b/Å	12.1202(3)	15.2154(3)	12.2478(3)	13.5072(2)	13.1750(1)
c/Å	22.0169(4)	16.3438(5)	13.1535(3)	13.9191(3)	61.8138(5)
α (°)	90	102.144(1)	96.180(1)	62.832(1)	90
β (°)	94.010(2)	98.439(1)	110.866(1)	80.910(1)	99.249(1)
γ (°)	90	111.559(1)	113.422(1)	68.659(1)	90
V/Å <sup>3</sup>	7062.3(3)	2635.21(12)	1530.93(6)	1720.36(5)	18938.5(3)
Z	4	1	1	1	12
D <sub>c</sub> /g cm <sup>-3</sup>	1.426	1.220	1.309	1.372	1.353
μ(Mo-Kα)	0.850	0.535	0.357	0.442	0.351
Total data	18 772	21 481	18 951	19 763	37 279
Unique data	4581	8901	6976	7847	14 306
R <sub>int</sub>	0.059	0.076	0.045	0.044	0.040
Observed data [I > 2σ(I)]	3760	7512	6232	6551	10 783
R <sub>1</sub> [I > 2σ(I)]	0.034	0.071	0.037	0.043	0.046
wR <sub>2</sub> (all data)	0.098	0.217	0.087	0.093	0.121
Goodness of fit, S	1.14	1.05	1.05	1.03	1.07
ρ <sub>min</sub> , ρ <sub>max</sub> e Å <sup>-3</sup>	-0.74, 0.69	-1.65, 1.18	-0.70, 0.45	-0.63, 0.35	-0.59, 0.45

**Fig. 4** Molecular units in the X-ray crystal structures of **P<sub>2</sub>-Rh3**, **P<sub>2</sub>-Rh5**, **P<sub>2</sub>-Ru2**, **P<sub>2</sub>-Ru3** and **P<sub>2</sub>-Ru4**. Displacement ellipsoids are shown at 30% probability and H atoms are omitted. All molecules lie on crystallographic inversion centres except **P<sub>2</sub>-Ru4** (mol2). For **P<sub>2</sub>-Ru4** (mol2), disorder of one phenyl substituent on dpap is not shown.**Table 4** Selected geometrical data (Å, °) for **P<sub>2</sub>-Rh3**, **P<sub>2</sub>-Rh5**, **P<sub>2</sub>-Ru2**, **P<sub>2</sub>-Ru3** and **P<sub>2</sub>-Ru4**. All molecules except **P<sub>2</sub>-Ru4** (mol2) lie on crystallographic inversion centres

	<b>P<sub>2</sub>-Rh3</b>	<b>P<sub>2</sub>-Rh5</b>	<b>P<sub>2</sub>-Ru2</b>	<b>P<sub>2</sub>-Ru3</b>	<b>P<sub>2</sub>-Ru4</b> (mol1)	<b>P<sub>2</sub>-Ru4</b> (mol2)
σ <sup>a</sup>	0.048	0.031	0.030	0.036	0.022	0.083
α <sup>b</sup>	86.4	89.1	87.7	88.8	88.6	89.8
β <sup>b</sup>						89.1
M–P1	2.3688(10)	2.3694(12)	2.3777(5)	2.3610(5)	2.3684(9)	2.3597(10)
M–P2						2.3784(10)
M–N1	2.051(3)	2.035(3)	2.0589(15)	2.0644(18)	2.056(3)	2.051(3)
M–N2	2.046(3)	2.041(4)	2.0561(15)	2.0638(17)	2.046(3)	2.048(3)
M–N3						2.060(3)
M–N4						2.059(3)

<sup>a</sup> σ denotes the average perpendicular deviation of the porphyrin core atoms from the least-squares plane through all 24 core atoms. <sup>b</sup> α and β denote the angle formed by the Rh–P1/P2 bond with the least-squares porphyrin plane.

## Experimental

### General

All manipulations were performed using standard inert atmosphere techniques, and freshly distilled and degassed solvents: methylene chloride (CH<sub>2</sub>Cl<sub>2</sub>), chloroform (CHCl<sub>3</sub>) from CaH<sub>2</sub>, methanol (MeOH) from Mg; CDCl<sub>3</sub> was filtered over basic alumina and degassed by purging with Ar prior to use. dpap (**1**), **Ru2** to **Ru5** and **Rh2** to **Rh5** have been synthesised as described elsewhere.<sup>19,31</sup> NMR spectra were recorded on a Bruker DPX400 NMR spectrometer at 400.13 MHz (<sup>1</sup>H, residual undeuterated solvent as internal standard) or 161.98 MHz (<sup>31</sup>P{<sup>1</sup>H}, H<sub>2</sub>PO<sub>4</sub> external standard); all spectra were recorded in CDCl<sub>3</sub> except for **P<sub>2</sub>Rh5** and **P<sub>2</sub>Ru5** (CDCl<sub>3</sub>-CD<sub>3</sub>OD 10:1). UV-vis spectra were recorded on a Varian Cary 100 Bio spectrophotometer. X-ray diffraction data were collected using a Nonius Kappa CCD diffractometer. Structures were solved by direct methods using either *SHELXS-97*<sup>36</sup> or *SIR-92*<sup>37</sup> and refined against all *F*<sup>2</sup> data using *SHELXL-97*.<sup>36</sup>

## General procedure for the synthesis of the complexes

The porphyrin (50 mg) was suspended in  $\text{CHCl}_3$  (5 ml), and neat dpap (5 eq.) was added. The solution was stirred at room temperature under an Ar atmosphere for 15 min., and the solvent was removed on a rotary evaporator. The residue was re-dissolved in 5 ml  $\text{CHCl}_3$ , stirred at room temperature for 10 min, then the solvent removed *in vacuo*. The orange solid was dissolved in a minimum amount of hot  $\text{CH}_2\text{Cl}_2$  (ca 2 ml), and 10 ml MeOH were carefully layered over the solution. After standing overnight, orange/bronze coloured crystals were collected on a sintered funnel, washed with MeOH and dried *in vacuo*. Yields are in the range of 90 to 98%. Crystals suitable for XRD analysis were grown from a saturated  $\text{CHCl}_3$  solution layered with MeOH.

**P<sub>2</sub>Rh2:** <sup>1</sup>H NMR  $\delta$  1.79 (t, 24H,  $J$  = 7.5 Hz, ethyl-CH<sub>3</sub>), 3.84 (m, 12H, ethyl-CH<sub>2</sub> and P-Ar-H<sub>o</sub>), 6.38 (t, 8H,  $J$  = 7.8 Hz, P-Ar-H<sub>m</sub>), 6.84 (t, 8H, 7.3 Hz, P-Ar-H<sub>p</sub>), 6.91 (d, 4H,  $J$  = 6.8 Hz, C $\equiv$ CAr-H<sub>o</sub>), 7.41 (t, 4H,  $J$  = 7.5 Hz, C $\equiv$ CAr-H<sub>m</sub>), 7.51 (t, 2H,  $J$  = 7.5 Hz, C $\equiv$ CAr-H<sub>p</sub>), 9.72 (s, 4H, H<sub>meso</sub>); <sup>31</sup>P NMR  $\delta$  -9.5 (d,  $J$  = 88 Hz). **P<sub>2</sub>Rh3:** <sup>1</sup>H NMR  $\delta$  1.66 (t, 12H,  $J$  = 7.3 Hz, ethyl-CH<sub>3</sub>), 2.26 (s, 12H,  $\beta$ -CH<sub>3</sub>), 3.73 (q, 8H,  $J$  = 7.3 Hz, ethyl-CH<sub>2</sub>), 3.98 (m, 8H, P-Ar-H<sub>o</sub>), 6.47 (t, 8H,  $J$  = 7.5 Hz, P-Ar-H<sub>m</sub>), 6.91 (t, 8H, 7.3 Hz, P-Ar-H<sub>p</sub>), 7.35 (m, 8H, Ar-H), 7.50 (m, 4H, Ar-H), 7.59 (t, 6H,  $J$  = 7.8 Hz, *meso*-Ar-H<sub>m,p</sub>), 7.76 (t, 2H,  $J$  = 7.5 Hz, C $\equiv$ CAr-H<sub>p</sub>), 9.76 (s, 2H, H<sub>meso</sub>); <sup>31</sup>P NMR  $\delta$  -9.8 (d,  $J$  = 89 Hz). **P<sub>2</sub>Rh4:** <sup>1</sup>H NMR  $\delta$  4.13 (q, 8H,  $J$  = 7.3 Hz, P-Ar-H<sub>o</sub>), 6.56 (t, 8H,  $J$  = 7.3 Hz, P-Ar-H<sub>m</sub>), 6.90 (d, 4H,  $J$  = 8.3 Hz, C $\equiv$ CAr-H<sub>o</sub>), 6.95 (t, 8H, 7.3 Hz, P-Ar-H<sub>p</sub>), 7.30 (m, 4H, C $\equiv$ CAr-H<sub>m</sub>), 7.44 (t, 2H,  $J$  = 7.3 Hz, C $\equiv$ CAr-H<sub>p</sub>), 7.64 (m, 20H, *meso*-Ar), 8.79 (s, 8H,  $\beta$ -H); <sup>31</sup>P NMR  $\delta$  -9.4 (d,  $J$  = 87 Hz). **P<sub>2</sub>Rh5:** <sup>1</sup>H NMR  $\delta$  4.19 (q, 8H,  $J$  = 7.3 Hz, P-Ar-H<sub>o</sub>), 5.32 (s, 72H <sup>1</sup>Bu), 6.58 (t, 8H,  $J$  = 7.2 Hz, P-Ar-H<sub>m</sub>), 6.87 (d, 4H,  $J$  = 7.1 Hz, C $\equiv$ CAr-H<sub>o</sub>), 6.96 (t, 8H, 7.4 Hz, P-Ar-H<sub>p</sub>), 7.16 (m, 4H, C $\equiv$ CAr-H<sub>m</sub>), 7.69 (d, 4H,  $J$  = 1.9 Hz, *meso*-Ar-H<sub>p</sub>), 7.81 (m, 8H, *meso*-Ar<sub>o</sub>), 8.85 (s, 8H,  $\beta$ -H); <sup>31</sup>P NMR  $\delta$  -8.2 (d,  $J$  = 85 Hz).

**P<sub>2</sub>Ru2:** <sup>1</sup>H NMR  $\delta$  1.61 (t, 12H,  $J$  = 7.4 Hz, ethyl-CH<sub>3</sub>), 3.68 (m, 8H, ethyl-CH<sub>2</sub>), 4.19 (m, 8H, P-Ar-H<sub>o</sub>), 6.29 (t, 8H,  $J$  = 7.6 Hz, P-Ar-H<sub>m</sub>), 6.63 (t, 8H, 7.6 Hz, P-Ar-H<sub>p</sub>), 6.98 (d, 4H,  $J$  = 7.2 Hz, C $\equiv$ CAr-H<sub>o</sub>), 7.30 (m, 4H, C $\equiv$ CAr-H<sub>m</sub>), 7.51 (t, 2H,  $J$  = 7.5 Hz, C $\equiv$ CAr-H<sub>p</sub>), 8.80 (s, 4H, H<sub>meso</sub>); <sup>31</sup>P NMR  $\delta$  -1.0. **P<sub>2</sub>Rh3:** <sup>1</sup>H NMR  $\delta$  1.53 (t, 12H,  $J$  = 7.8 Hz, ethyl-CH<sub>3</sub>), 1.55 (s, 12H,  $\beta$ -CH<sub>3</sub>), 3.56 (q, 8H,  $J$  = 7.4 Hz, ethyl-CH<sub>2</sub>), 4.42 (m, 8H, P-Ar-H<sub>o</sub>), 6.41 (t, 8H,  $J$  = 7.5 Hz, P-Ar-H<sub>m</sub>), 6.71 (t, 4H, 7.0 Hz, P-Ar-H<sub>p</sub>), 7.01 (d, 4H,  $J$  = 8.3 Hz, C $\equiv$ CAr-H<sub>o</sub>), 7.29 (m, 6H, Ar-H), 7.40 (m, 6H, Ar-H), 7.54 (m, 2H, Ar-H), 8.80 (s, 2H, H<sub>meso</sub>); <sup>31</sup>P NMR  $\delta$  2.0. **P<sub>2</sub>Rh4:** <sup>1</sup>H NMR  $\delta$  4.57 (m, P-Ar-H<sub>o</sub>), 6.50 (t, 8H,  $J$  = 7.5 Hz, P-Ar-H<sub>m</sub>), 6.77 (t, 8H, 7.3 Hz, P-Ar-H<sub>p</sub>), 6.99 (d, 4H,  $J$  = 8.3 Hz, C $\equiv$ CAr-H<sub>o</sub>), 7.16 (t, 4H,  $J$  = 7.5 Hz, C $\equiv$ CAr-H<sub>m</sub>), 7.27 (t, 2H,  $J$  = 7.3 Hz, C $\equiv$ CAr-H<sub>p</sub>), 7.46 (t, 8H,  $J$  = 7.8 Hz, *meso*-Ar<sub>m</sub>), 7.54 (t, 4H,  $J$  = 7.3 Hz, *meso*-Ar<sub>p</sub>), 7.60 (d, 8H,  $J$  = 6.8 Hz, *meso*-Ar<sub>o</sub>), 8.13 (s, 8H,  $\beta$ -H); <sup>31</sup>P NMR  $\delta$  0.2. **P<sub>2</sub>Rh5:** <sup>1</sup>H NMR  $\delta$  4.57 (q, 8H,  $J$  = 7.3 Hz, P-Ar-H<sub>o</sub>), 5.30 (s, 72H <sup>1</sup>Bu), 6.48 (t, 8H,  $J$  = 7.5 Hz, P-Ar-H<sub>m</sub>), 6.74 (t, 8H, 7.4 Hz, P-Ar-H<sub>p</sub>), 6.95 (d, 4H,  $J$  = 9.1 Hz, C $\equiv$ CAr-H<sub>o</sub>), 7.05 (t, 4H,  $J$  = 7.7 Hz, C $\equiv$ CAr-H<sub>m</sub>), 7.15 (t, 2H,  $J$  = 10.1 Hz, C $\equiv$ CAr-H<sub>p</sub>), 7.34 (m, 8H, *meso*-Ar-H<sub>o,m</sub>), 7.65 (m, 4H, *meso*-Ar<sub>p</sub>), 8.17 (s, 8H,  $\beta$ -H); <sup>31</sup>P NMR  $\delta$  3.0.

## Notes and references

- C. M. Che and J. S. Huang, *Chem. Commun.*, 2009, 3996–4015.
- C. M. Che, J. L. Zhan, R. Zhang, J. S. Huang, T. S. Lai, W. M. Tsui, X. G. Zhou, Z. Y. Zhou, N. Y. Zhu and C. K. Chang, *Chem.–Eur. J.*, 2005, **11**, 7040–7053.
- G. Jiang, J. Chen, H.-Y. Thu, J.-S. Huang, N. Zhu and C.-M. Che, *Angew. Chem., Int. Ed.*, 2008, **47**, 6638–6642.
- S. Fantauzzi, A. Caselli and E. Gallo, *Dalton Trans.*, 2009, 5434–5443.
- C. Y. Zhou, W. Y. Yu and C. M. Che, *Org. Lett.*, 2002, **4**, 3235–3238.
- M. S. Rodriguez-Morgade, M. E. Plonska-Brzezinska, A. J. Athans, E. Carbonell, G. de Miguel, D. M. Guldi, L. Echegoyen and T. Torres, *J. Am. Chem. Soc.*, 2009, **131**, 10484–10496.
- J. Xie, J.-S. Huang, N. Zhu, Z.-Y. Zhou and C.-M. Che, *Chem.–Eur. J.*, 2005, **11**, 2405–2416.
- J. S. Huang, G. A. Yu, J. Xie, K. M. Wong, N. Y. Zhu and C. M. Che, *Inorg. Chem.*, 2008, **47**, 9166–9181.
- X. Zhou, M. K. Tse, D. D. Wu, T. C. W. Mak and K. S. Chan, *J. Organomet. Chem.*, 2000, **598**, 80–86.
- M. S. Sanford and J. T. Groves, *Angew. Chem., Int. Ed.*, 2004, **43**, 588–590.
- K. Kajiyama, T. K. Miyamoto and K. Sawano, *Inorg. Chem.*, 2006, **45**, 502–504.
- I. Bouamaied, T. Coskun and E. Stulz, in *Structure & Bonding*, ed. E. Alessio, Springer, Heidelberg, 2006, pp. 1–48.
- E. Stulz, S. M. Scott, A. D. Bond, S. Otto and J. K. M. Sanders, *Inorg. Chem.*, 2003, **42**, 3086–3096.
- E. Stulz, J. K. M. Sanders, M. Montalti, L. Prodi, N. Zaccaroni, F. de Biani, E. Grigiotti and P. Zanello, *Inorg. Chem.*, 2002, **41**, 5269–5275.
- E. Stulz, M. Maue, N. Feeder, S. J. Teat, Y. F. Ng, A. D. Bond, S. Darling and J. K. M. Sanders, *Inorg. Chem.*, 2002, **41**, 5255–5268.
- B. G. Maiya, N. Bampos, A. A. Kumar, N. Feeder and J. K. M. Sanders, *New J. Chem.*, 2001, **25**, 797–800.
- J. E. Redman, N. Feeder, S. J. Teat and J. K. M. Sanders, *Inorg. Chem.*, 2001, **40**, 2486–2499.
- J. E. Redman, N. Feeder, S. J. Teat and J. K. M. Sanders, *Inorg. Chem.*, 2001, **40**, 3217–3221.
- E. Stulz, S. M. Scott, Y. F. Ng, A. D. Bond, S. J. Teat, S. L. Darling, N. Feeder and J. K. M. Sanders, *Inorg. Chem.*, 2003, **42**, 6564–6574.
- S. L. Darling, E. Stulz, N. Feeder, N. Bampos and J. K. M. Sanders, *New J. Chem.*, 2000, **24**, 261–264.
- E. Stulz, M. Maue, S. M. Scott, B. E. Mann and J. K. M. Sanders, *New J. Chem.*, 2004, **28**, 1066–1072.
- E. Stulz, S. M. Scott, A. D. Bond, S. J. Teat and J. K. M. Sanders, *Chem.–Eur. J.*, 2003, **9**, 6039–6048.
- E. Stulz, Y.-F. Ng, S. M. Scott and J. K. M. Sanders, *Chem. Commun.*, 2002, 524–525.
- H. Xu and D. K. P. Ng, *Inorg. Chem.*, 2008, **47**, 7921–7927.
- K. Funatsu, A. Kimura, T. Imamura, A. Ichimura and Y. Sasaki, *Inorg. Chem.*, 1997, **36**, 1625–1635.
- K. Funatsu, T. Imamura, A. Ichimura and Y. Sasaki, *Inorg. Chem.*, 1998, **37**, 4986–4995.
- K. Funatsu, T. Imamura, A. Ichimura and Y. Sasaki, *Inorg. Chem.*, 1998, **37**, 1798–1804.
- K. Fukushima, K. Funatsu, A. Ichimura, Y. Sasaki, M. Suzuki, T. Fujihara, K. Tsuge and T. Imamura, *Inorg. Chem.*, 2003, **42**, 3187–3193.
- M. J. Gunter and K. M. Mullen, *Inorg. Chem.*, 2007, **46**, 4876–4886.
- K. M. Mullen and M. J. Gunter, *J. Org. Chem.*, 2008, **73**, 3336–3350.
- A. J. Carty, N. K. Hota, T. W. Ng, H. A. Patel and T. J. O'Connor, *Can. J. Chem.*, 1971, **49**, 2706–2711.
- O. Q. Munro, G. L. Camp and L. Carlton, *Eur. J. Inorg. Chem.*, 2009, 2512–2523.
- C. J. Medforth, C. M. Muzzi, K. M. Shea, K. M. Smith, R. J. Abraham, S. L. Jia and J. A. Shelnutz, *J. Chem. Soc., Perkin Trans. 2*, 1997, 839–844.
- C. J. Medforth, C. M. Muzzi, K. M. Shea, K. M. Smith, R. J. Abraham, S. L. Jia and J. A. Shelnutz, *J. Chem. Soc., Perkin Trans. 2*, 1997, 833–837.
- E. Steiner and P. W. Fowler, *ChemPhysChem*, 2002, **3**, 114–116.
- G. M. Sheldrick, University of Göttingen, Germany.
- A. Altomare, G. Casciarano, C. Giacovazzo, A. Guagliardi, M. C. Burla, G. Polidori and M. Camalli, *J. Appl. Cryst.*, 1994, **27**, 435–436.